Journal of Hazardous Materials 497 (2025) 139614

Contents lists available at ScienceDirect

Journal of Hazardous Materials

journal homepage: www.elsevier.com/locate/jhazmat

Unraveling micro/nanoplastics and phthalates in infusion solutions: A novel integrated approach for quantification and cardiovascular cytotoxicity evaluation

Xue Zhang [a,1], Ruqin Shen [a,b,1], Peng Xia [a], Hongli Tan [c], Yongfeng Deng [a,*]

[a] Key Laboratory of Environmental Medicine Engineering, Ministry of Education, School of Public Health, Southeast University, Nanjing 210009, China
[b] Department of Environmental Science and Engineering, Fudan University, Shanghai 200438, China
[c] Guangdong Engineering Research Center of Chinese Medicine & Disease Susceptibility, School of Traditional Chinese Medicine, Jinan University, Guangzhou 510632, China

HIGHLIGHTS

- The CPE and Py-TD-GC/MS union enables accurate quantification of MNPs.
- PE, PP, and PS MNPs are widely present in infusions.
- NPs are significantly more prevalent than MPs.
- PP and PE MNPs significantly positively correlated with DBzP and DEHP.
- Co-exposure to PS-NPs and DEHP exhibits synergistic toxicity.

GRAPHICAL ABSTRACT

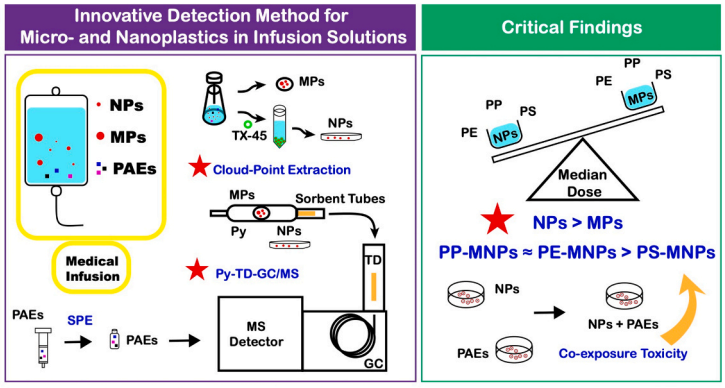

ARTICLE INFO

Keywords:
Infusion
Micro/Nanoplastics
Phthalates
Cloud-point extraction

ABSTRACT

Infusion therapy represents a critical and emerging exposure pathway for micro/nanoplastics (MNPs), with significant implications for human health. However, accurate and simultaneous analytical methods for MNPs in infusion solutions are still underdeveloped, and the potential co-exposure to MNPs and phthalates (PAEs) has not been fully explored. This study presents a novel integrated analytical approach combining Cloud-Point Extraction with Pyrolysis-Thermal Desorption-Gas Chromatography-Mass Spectrometry, enabling efficient extraction and

List of abbreviations: BMPP, Bis4-Methylpentyl phthalate; Caspase-3, Cysteinyl aspartate specific proteinase-3; CPE, Cloud point extraction; DAmP, Diamyl phthalate; DBP, Dibutyl phthalate; DBzP, Dibenzyl phthalate; DEHP, Bis2-ethylhexyl phthalate; DEP, Diethyl Phthalate; DHP, Dihexyl phthalate; DIBP, Diisobutyl phthalate; DMP, Dimethyl phthalate; DPhP, Diphenyl phthalate; GC, Gas chromatography; HUVECs, Human umbilical vein endothelial cells; ITGA4, Integrin Subunit Alpha 4; MNPs, Micro/nanoplastics; MPs, Microplastics; NAT, Nanoparticle tracking analysis; NPs, Nanoplastics; PE, Polyethylene; PET, Polyethylene terephthalate; PPARγ, Peroxisome Proliferator Activated Receptor Gamma; PP, Polypropylene; PS, Polystyrene; PVC, Polyvinyl chloride; Py, Pyrolysis; TD, Thermal desorption; TEM, Transmission electron microscopy; TX-45, Triton X-45.

* Corresponding author.
E-mail address: yfdeng@seu.edu.cn (Y. Deng).
[1] Xue Zhang, and Ruqin Shen contributed equally to this work.

https://doi.org/10.1016/j.jhazmat.2025.139614
Received 24 February 2025; Received in revised form 1 August 2025; Accepted 19 August 2025
Available online 22 August 2025

Py-TD-GC/MS
Co-exposure toxicity

precise quantification of MNPs from commonly used glucose and saline infusions, with MNP recovery rates ranging from 96.74 % to 108.25 %. Our results reveal the presence of Polyethylene (PE), Polypropylene (PP) and Polystyrene (PS) MMPs are present in PP-based infusion, with median concentrations from 30.45 to 125.27 μg/L. Notably, nanoplastics (NPs) dominate, with PE-, PP-, and PS-NPs detected at median concentrations of 29.09 and 87.54 μg/L. Additionally, ten different PAEs were identified, with a significant positive correlation between Diamyl phthalate and Bis(2-ethylhexyl) phthalate and MNPs. Co-exposure to PS-NPs and DEHP further demonstrates the synergistic toxic effects in vitro. These findings highlight the pervasive contamination of infusions by MNPs and PAEs, underscoring the urgent need for enhanced regulatory measures and advanced technologies to mitigate the health risks associated with these contaminants in medical products.

1. Introduction

Recent research increasingly indicates that microplastics (MPs) have infiltrated various human tissues and bodily fluids, including the liver, lungs, intestines, blood vessels, feces, and cerebrospinal fluid [1,2]. Simultaneously, several epidemiological studies suggest that MPs may increase the risk of cardiovascular diseases and intestinal inflammation [3,4]. Classic animal exposure models have shown that when micro/-nanoplastics (MNPs) enter the body, they can significantly disrupt metabolic, digestive, immune, neurological, and reproductive functions, potentially inducing a range of diseases [5,6]. Compared to MPs, the toxicity of nanoplastics (NPs) has attracted more attention due to their smaller size, which theoretically allows them to penetrate a wider array of tissues and bodily fluids [7]. While direct evidence linking MNPs to the initiation and progression of diseases remains limited, the potential health risks associated with these plastic particles remain a major research focus [8], especially as separation and detection technologies for MNPs improve [9].

The unique route of MNP exposure via intravenous infusion potentially presents more significant health risks compared to conventional oral, inhalation, or dermal pathways [10]. This is primarily because MNPs introduced through infusion bypass the typical absorption and transport barriers, directly entering the bloodstream, where they can be distributed throughout the body, potentially causing multi-organ damage, such as blocking blood vessels and stroke [11,12]. In contrast, the majority of MNPs ingested orally, inhaled, or absorbed through the skin are generally hindered by various biological barriers, such as the intestinal epithelium, alveolar epithelium, and dermal layers, and are eventually excreted via bodily fluids or feces [13]. Importantly, the growing use of plastic materials for infusion packaging, driven by logistical, cost, and convenience factors, substantially increases the likelihood of MNPs entering the systemic circulation via intravenous infusion [10,14]. Several recent studies have revealed the presence of MNPs in commonly used infusion bags. For instance, Cui et al. [15] employed Fourier-transform infrared spectroscopy and detected MPs ranging from 15 to 100 μm in size in infusion fluids, with concentrations of 2.91 ± 3.91 particles per liter. Similarly, Zhu et al. [16] used Raman microscopy to identify MPs ranging from 4 to 148 μm in infusion solutions, with a concentration of 1–2 particles per bag. More recently, Huang et al. [10] combined surface-enhanced Raman spectroscopy and scanning electron microscopy to identify MPs with a size range of 1–62 μm, with concentrations as high as 7500 particles per liter. These findings not only underscore the considerable potential for MNPs to be introduced into the systemic circulation via intravenous infusion, but also emphasize the importance of advanced detection techniques in accurately quantifying the true content of MNPs in infusion solutions.

Despite notable advancements in analytical techniques, accurately and simultaneously quantifying MNPs in intravenous infusion fluids remains a substantial challenge. Traditional spectroscopic methods are typically limited to semi-quantitative analysis of larger MPs (4–148 μm), due to the diffraction limitations inherent to spectroscopic techniques [15,16]. These limitations prevent the accurate detection of smaller particles, particularly those below 10 μm, and especially those under 5 μm [17,18]. Although combining spectroscopic techniques with electron scanning microscopy can significantly improve the detection sensitivity for smaller microplastics (1–10 μm), these methods are still inadequate for the identification and quantification of NPs [10]. As a result, spectroscopic-based approaches tend to underestimate the concentration of MNPs in infusion solutions, particularly missing the abundant NPs present. In contrast, the analytical techniques such as pyrolysis (Py), thermal desorption (TD), and gas chromatography-mass spectrometry (GC-MS) hold considerable promise for overcoming the particle size limitations and enabling the absolute quantification of MNPs. For instance, Wang et al. [14] successfully employed these techniques to quantify NPs in infusion solutions for the first time. However, their study reported low recovery rates for MNPs, ranging from 15.6 % to 31.6 %, which is significantly lower than recovery rates observed in similar analyses of MNPs in other environmental matrices or biological samples [17,19]. This discrepancy underscores the need for further optimization of extraction and quantification methods specific to infusion fluids.

The low recovery rates are likely attributed to suboptimal sample preparation methods, particularly in the extraction and enrichment of MPs and NPs from complex infusion matrices [20]. In contrast, cloud point extraction (CPE) offers advantages due to its temperature-induced phase separation, heightened sensitivity to the surface characteristics of MNPs, and effective mitigation of matrix interferences [21]. Additionally, the use of surfactants, coupled with their strong affinity for NPs, enhances the selectivity and enrichment efficiency of this technique in complex biological and chemical matrices [22]. Therefore, an integrated approach combining cloud point extraction with advanced Py-TD-GC/MS has the potential to significantly improve the extraction and quantification of MPs and NPs in infusions, contributing to more precise risk assessments and mitigation strategies for MNPs exposure in medical and public health contexts.

Furthermore, combined exposure to MNPs and toxic plasticizers may result in even more severe health effects. Previous studies have shown that combined exposure to MPs and phthalates (PAEs) can significantly worsen intestinal or reproductive toxicity compared to individual exposure [23,24]. Importantly, plastic infusion bags, commonly used in medical settings, present a unique risk due to their potential to release both plastic particles and plasticizers. However, fewer studies have yet comprehensively investigated the types and concentrations of MNPs and PAEs released simultaneously from plastic infusion bags, further hindering the understanding of the synergistic health effects of this combined exposure in medical contexts.

In this study, we hypothesize that plastic infusion bags can simultaneously release MNPs and PAEs into the human circulatory system. To test this hypothesis, we have developed an innovative method combining CPE with Py-TD-GC/MS for the extraction and quantification of MNPs and common PAEs from large-volume infusion solutions. This methodology enables precise assessment of the concentrations and distribution patterns of MNPs and PAEs in commonly used saline and glucose infusion bags. Additionally, we also explore whether co-exposure to NPs and PAEs results in synergistic toxic effects by a vitro model. The results of this study will provide important insights into the identification and evaluation of health risks posed by MNPs and plastic additives in medical products, offering valuable directions for improving global plastic pollution control and advancing the quality assurance of

medical products in the future.

2. Methods and materials

2.1. Chemicals and reagents

Three plastic standards (Polyethylene, PE; Polypropylene, PP; and Polystyrene, PS) were purchased from Sigma-Aldrich Inc. (St. Louis, MO. UAS). The standard samples of PE, PP, and PS used in this study had particle sizes of less than 70 μm. This size range was selected because recent studies have reported MNPs within a similar size distribution in infusion products [10,14,16]. Ten phthalate standards, including Bis (4-Methylpentyl) phthalate (BMPP), Diamyl phthalate (DAmP), Dibutyl phthalate (DBP), Dibenzyl phthalate (DBzP), Bis(2-ethylhexyl) phthalate (DEHP), Diethyl Phthalate (DEP), Dihexyl phthalate (DHP), Diisobutyl phthalate (DIBP), Dimethyl phthalate (DMP), and Diphenyl phthalate (DPhP) were obtained from Dr. Ehrenstorfer GmbH (Augsburg, Freistaat Bayern, Germany), and all purities were > 98 %. Two isotope-labelled including Phthalic acid, bis-hexyl ester-d4 (DHP-d4) and Phthalic acid, bis-2-ethylhexyl ester-d4 (DEHP-d4) were from Dr. Ehrenstorfer GmbH (Augsburg, Freistaat Bayern, Germany), and all purities were > 96.78 %. Triton X-45 (TX-45) was purchased from Sigma-Aldrich Inc. (St. Louis, MO. UAS). The extraction solvents were all of high-performance liquid chromatography grade, sourced from Fisher Chemical (USA). Solid phase extraction columns (Poly-Sery HLB, 500 mg/6 mL) were obtained from CNW Technologies GmbH (CNW ANPEL, Shanghai, China). Ultrapure water (> 18 MΩ) produced with a Milli- Q gradient system (Millipore, Billerica, MA) was used throughout the experiments.

2.2. Sample collection

To ensure the relevance of this study to real-world human exposure scenarios, saline (0.9 % sodium chloride solution) and glucose (5 %) infusion solutions, two of the most widely used medical solutions globally, were chosen as the focus. Six brands of saline and three brands of glucose solutions from two different batches were collected, all sourced directly from hospitals across three cities in China, to better reflect the consistency of MNP levels in these solutions. Detailed information on sampling is provided in Table S1 of the supplementary materials. Additionally, to further assess the potential plastic aging and MNP release during the storage of infusion solutions, we also recorded the storage conditions and durations at each hospital (Table S2), and a batch of samples was stored under real-world conditions and durations (dark storage at 24 °C for 28 days) for subsequent analysis. Raman spectroscopy (XploRA PLUS, HORIBA, France) was employed to characterize the polymer composition of the plastic packaging for all infusion packages. The aging of plastic packaging was evaluated using Two-dimensional correlation spectroscopy (2D-COS) analysis, with detailed methods provided in the supplementary materials.

2.3. MPs and NPs extraction

To minimize contamination from external plastic particles, the outer surfaces of the packaging bags were thoroughly cleaned with ultrapure water prior to opening. The packaging bags were carefully opened using sterilized metal scissors, and the solutions were transferred and then extracted under controlled conditions to isolate MPs, NPs, and potential additives, respectively. For MP collection, 100 mL of glucose or saline infusion was filtered through a pre-cleaned 1 μm glass fiber membrane (Whatman, United States). The membranes were subsequently dried and stored for further MP analysis (Fig. 1).

To isolate NPs, a modified CPE method was employed [21,22]. Specifically, 40 mL of the solution was mixed with 400 μL of 1 M $MgSO_4$ solution and 120 μL of 10 % (w/v) TX-45 solution. The mixture was vortexed thoroughly (1000 rpm, 15 min) and incubated in a water bath at 45°C for 15 min. Following incubation, the sample was centrifuged at 4000 rpm at −4°C for 20 min to obtain the surfactant-rich phase. The TX-45 phase, containing the enriched NPs, was carefully transferred into a quartz sample boat. The TX-45 was evaporated at 170°C for 4 h, leaving the NPs ready for subsequent quantitative analysis (Fig. 1).

2.4. Plastic additive extraction

Saline and glucose solution samples were initially filtered through a pre-cleaned 0.45 μm fiber membrane (Whatman, United States). A 100-mL aliquot of the filtered solution was then spiked with 100 ng of two internal standards before extraction. For solid-phase extraction, Poly-

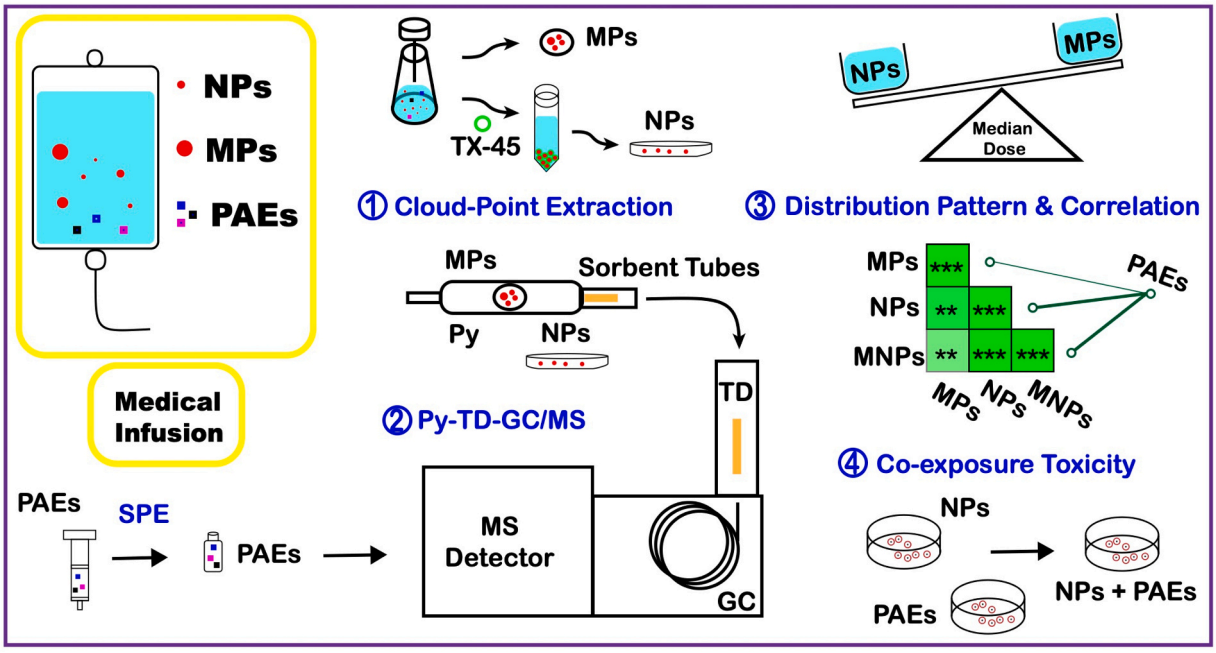

Fig. 1. Schematic of the separation and detection process for microplastics (MPs), nanoplastics (NPs), and phthalates (PAEs).

Sery HLB cartridges were preconditioned sequentially with 5 mL of methanol followed by 5 mL of ultrapure water. The spiked solution samples were passed through the preconditioned cartridges at a controlled flow rate of 5 mL·min^{-1} . Subsequently, the cartridges were rinsed with 5 mL of ultrapure water and then dried under vacuum for 30 min to eliminate any remaining moisture. The target analytes were eluted with 10 mL of methanol, and the resulting extracts were evaporated to dryness under a gentle nitrogen stream at 30°C. Finally, the dried extracts were reconstituted in 1 mL of hexane for subsequent analysis using GC/MS (Fig. 1).

2.5. MPs and NPs detection

We employed an integrated Py-TD-GC/MS for MP and NP detection. The analytical workflow comprised three key processes: pyrolysis of MP- or NP-enriched samples, thermal desorption of MP or NP pyrolysis products, and MP or NP quantification via GC/MS (Fig. 1).

2.5.1. Pyrolysis

MP and NP-enriched samples were subjected to pyrolysis using a standalone tube furnace (Siyang Precision Equipment Co., Ltd., Shanghai, China). The furnace was programmed to heat from 100 °C to 550 °C at a rate of 50 °C·min^{-1} , maintained at 550 °C for 15 min, and then cooled back to 100 °C. During pyrolysis, a continuous nitrogen flow (100 mL·min^{-1}) was used to carry the pyrolysis products from the sample to a Tenax-TA sorbent tube (Kaver Scientific Instruments Ltd., Nanjing, China) for subsequent analysis.

2.5.2. Thermal desorption

The Tenax-TA sorbent tubes were subjected to thermal desorption using a thermal desorption system (Taitong Technology Co., Ltd., Guangzhou, China). Complete desorption was achieved at 300 °C for 10 min with a continuous nitrogen flow of 50 mL·min^{-1} . The desorbed products were initially trapped in a cold trap unit maintained at 30 °C for 1 min, followed by rapid heating to 300 °C, which was sustained for 4 min under the nitrogen flow conditions (50 mL·min^{-1}).

2.5.3. GC/MS

The desorbed products from the cold trap were analyzed using a GC/MS system consisting of a 7890B GC coupled with a 5977B MS (Agilent Technologies, CA, USA). Compound separation was achieved with a DB-624 column (250 μm × 1.4 μm × 30 m) using high-purity helium as the carrier gas at a flow rate of 1.5 mL·min^{-1} . The column oven temperature was programmed to increase from 35 °C (held for 5 min) to 260 °C at a rate of 10 °C·min^{-1} and maintained at 260 °C for 10 min. Mass spectrometric detection was performed in full-scan mode (m/z 35–350) with electron impact ionization at 70 eV, an ion source temperature of 230 °C, and a quadrupole temperature of 150 °C. PE, PP and PS were identified based on their characteristic pyrolysis decomposition products and corresponding retention times (Table S3). Quantification of target polymers was achieved through external calibration curves established using standard materials.

2.5.4. Nanoparticle tracking analysis (NTA)

To further cross-validate the nanoparticle content in infusion solutions, particularly focusing on particle count concentration, we continued using NTA to investigate the non-dissolved nanoparticles in two types of infusion solutions, both in their original state and after storage under real-world conditions. The specific NTA detection methods are detailed in the supplementary materials.

2.6. PAE detection

The detection and quantification of ten phthalate esters (PAEs) were performed using a GC/MS system comprising an 8890 GC coupled with a 7250 MS (Agilent Technologies, CA, USA). Separation was achieved using an Agilent 19091S-431UI column (250 μm × 0.25 μm × 50 m) with high-purity helium as the carrier gas at a flow rate of 1.5 mL·min^{-1} . The column oven temperature was programmed as follows: an initial hold at 30 °C for 0.5 min, followed by a ramp to 160 °C at 30 °C·min^{-1} , then to 315 °C at 15 °C·min^{-1} , with a final hold at 315 °C for 5 min. Mass spectrometric detection conditions, including ionization voltage, source temperature, and full-scan mode (m/z range), were identical to those described for the plastic particle detection method [25].

2.7. Quality assurance and quality control

To prevent background contamination for obtaining reliable data, the experimental procedures, including sampling, treatment, and recovery efficiency assessments, were conducted under a “plastic-free” protocol [17,26]. Glassware used during the simulation and filtration processes was pre-cleaned and baked at 500 °C for 3 h, then immediately covered with aluminum foil. The reagents used in this study were filtered using pre-calcined glass fiber filters with a pore size of 0.3 μm. Researchers wore cotton clothing and powder-free nitrile gloves to avoid contamination. Procedural blank samples were included in each batch to monitor and eliminate background contamination.

Spike recovery experiments were conducted to evaluate the accuracy of polymer and PAE quantification from digestion to detection. In addition, the matrix effect of the infusion solutions was also assessed through spiking experiments. Calibration curves were constructed by plotting the chromatographic peak areas of specific marker compounds. The mass of the target compound in the samples was calculated using these calibration curves. To assess analytical reproducibility, representative samples were analyzed in technical triplicates and re-evaluated on three non-consecutive days. Relative standard deviations were consistently below 5 % across both intra- and inter-day measurements, demonstrating high precision and methodological stability. All results are presented after subtracting the background values in this study.

2.8. Evaluation of cellular toxicity induced by Co-exposure NPs and PAEs

2.8.1. Cell culture and treatment

Human umbilical vein endothelial cells (HUVECs) were purchased from the National Collection of Authenticated Cell Cultures (Shanghai, China), and maintained in Dulbecco’s modified Eagle’s medium (Gibco, CA, USA) supplemented with 10 % fetal bovine serum (Gibco, CA, USA), and 1 % penicillin and streptomycin (Gibco, CA, USA) at 37 °C in a 5 % CO_2 atmosphere. HUVECs cells (7 ×10^3 cells/well) were seeded in 96-well culture plates for 24 h, followed by treatment with 50 nm PS-NPs (Biotyscience, China), DEHP (B&K, China), or their combination. The PS-NPs were characterized in terms of their morphology, particle size distribution, and material composition (Figure S1). For PS-NPs treatment, the concentration gradients of PS-NPs were as follow: 0, 6.25, 12.5, 25, 50, 100, 200, 400, 800, 1600 μg/mL. For DEHP treatment, the concentration gradients of PS-NPs were as follow: 0, 35, 70, 140, 280, 350, 560, 1120, 2240 ng/mL. For their combined toxicity, the exposure groups including PS-NPs groups (50 and 100 μg/mL), DEHP groups (35 and 70 ng/mL), and their combination (The low exposure: 50 μg/mL PS-NPs + 35 ng/mL DEHP; The high exposure: 100 μg/mL PS-NPs + 70 ng/mL DEHP). The selection of PS-NPs, DEHP, and their combined exposure concentrations was based on established cytotoxicity data for NPs and phthalates from previous studies [27,28], as well as their relative concentrations measured in infusion solutions.

2.8.2. Cell viability analysis

After a 24-hour exposure, the culture medium was removed from the sample wells. Subsequently, 100 μL of a 10 % CCK-8 solution (Abbkine, China) was added to each well. The plates were then incubated at 37°C for 30 min. Absorbance was measured at 450 nm using a microplate reader (Biotek, USA). Cell viability was calculated as a percentage relative to the untreated control cells.

2.8.3. Quantitative real-time polymerase chain reaction (qPCR)

To explore the synergistic toxicity of combined exposure to NPs and PAEs, this study focused on the quantitative analysis of three genes, including *Caspase-3* (Cysteine-aspartic protease 3), *PPARγ* (Peroxisome Proliferator-Activated Receptor Gamma), and *ITGA4* (Integrin Alpha 4), which play pivotal roles in inflammation, lipid metabolism, and apoptosis [29-31]. The primers used for the amplification of these genes (Table S4), along with the specific qPCR protocol, are detailed in the Supplementary Materials.

2.9. Statistical analysis

Statistical analyses were conducted using R version 4.3. Data normality was assessed via the Shapiro-Wilk test. Based on the results of the normality test, differences in MP, NP, and PAE levels among the two groups were evaluated using either the Student's *t*-test (for normally distributed data) or the Mann-Whitney *U* test (for non-normal distributions). Results were reported as mean ± standard deviation (SD). Associations between MPs, NPs, and PAEs were explored using Spearman correlation analysis and the Mantel test in R with the linkET package. Statistical significance was defined as $p < 0.05$.

3. Results and discussion

In contrast to traditional glass infusion bottles, plastic infusion bags offer numerous advantages, including lightness, flexibility, and cost-efficiency, making them widely adopted for infusion containers. Common plastics used in these bags, such as polyethylene (PE), Polyvinyl chloride (PVC), and PP, are chemically stable and resistant to reactions with the active ingredients in the infusions, ensuring the preservation of the drug's integrity and stability throughout the infusion process. Here, the Raman spectroscopy analysis conducted in this study revealed highly consistent spectra across infusion packaging from 6 brands of saline solution and 3 brands of glucose solution (Fig. 2). Key characteristic peaks were observed at 808, 841, 1152, 1326, and 1457 cm^{-1} (Fig. 2), which were directly correlated with known spectral features of PP plastics [32,33]. Specifically, these peaks were attributed to C-C stretching, CH3 rocking, C-C stretching, CH2 twisting, and CH2 bending vibrational modes. Consequently, it can be confidently concluded that the plastic infusion bags selected for this study were made from PP, a finding consistent with a recent report [16].

This study subsequently primarily focuses on MNPs derived from PE, PP and PS, three plastics commonly found in medical infusion solutions.

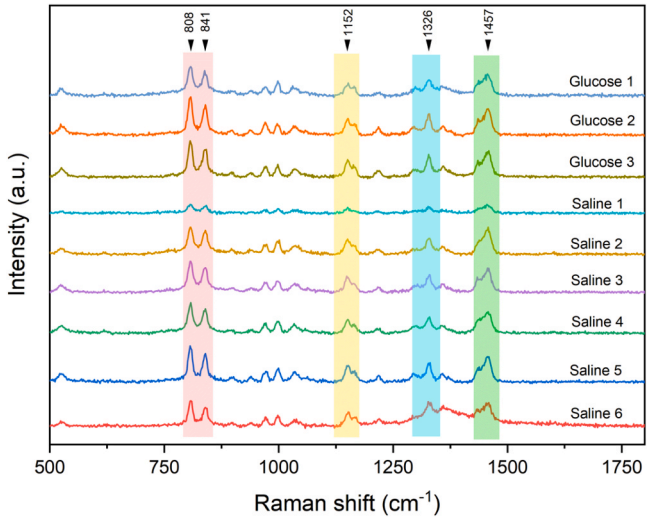

Fig. 2. Qualitative analysis of packaging materials for nine brands of saline and glucose infusion solutions using Raman spectroscopy.

Firstly, PP is the predominant material used in the packaging of the infusion solutions analyzed in this study, making it the most relevant plastic for detection. PE and PS, though not a major component of infusion packaging, was chosen as a representative of external contamination due to its widespread detection in various environmental media and biological samples, including human liver and blood [34]. More importantly, PS has been shown to be efficiently concentrated using the CPE method [21], significantly enhances the reliability and consistency of the results. This methodological advantage made PS a suitable target for investigation in this study. Furthermore, PE and PS, particularly in their NP form, have been extensively studied in toxicological research, with numerous studies highlighting their significant toxicity [34].

3.1. Method validation: procedure blanks and spiking recovery

To ensure the accuracy and sensitivity of the analytical methods, comprehensive procedural blanks were established throughout the workflow. The procedural blank results for MNPs revealed a 100 % detection rate for both PE, PP and PS particles, with concentrations of PE-MPs, PP-MPs and PS-MPs recorded at 0.17 ± 0.15, 1.02 ± 0.79 and 0.09 ± 0.07 μg, respectively. Additionally, we also provide for the first time detailed data on the baseline contamination levels of PE-NPs, PP-NPs and PS-NPs during laboratory-based NP separation procedures, with detected concentrations of 1.90 ± 0.82, 2.99 ± 0.21 and 0.28 ± 0.01 μg. These findings reveal the ubiquitous contamination of laboratory environments by MNPs, with background levels of NPs markedly surpassing those of MPs.

These results agree with those from contemporaneous studies, highlighting the difficulty of completely avoiding plastic contamination in laboratory settings [35]. Despite efforts to minimize the use of plastic products in MNP detection, the presence of various plastic equipment and materials in the laboratory inevitably leads to contamination. For example, Zhu et al. [36] reported average procedural blank concentrations of 0.235 μg and 0.803 μg for PP-MPs and PS-MPs when analyzing MPs in human feces and urine using TD-GC/MS. These findings demonstrate that the background control of MPs in this study is comparable to that reported in contemporaneous high-quality research. Importantly, the background concentrations of NPs were higher than those of MPs, suggesting that, beyond conventional sources, routine laboratory solvents may represent a significant additional pathway for NP introduction. For example, Liu et al. [37] similarly found MPs and NPs in digestion reagents such as hydrogen peroxide and potassium hydroxide solutions, with NPs being present in higher concentrations than MPs, and PP-NP levels (i.e., 3.33–43.01 mg/kg) being particularly abundant. Nonetheless, sustained efforts to reduce background contamination will be essential, including the establishment of purpose-built, plastic-free laboratories dedicated to the accurate analysis of MNPs.

The recovery rates for MNPs (PE, PP, and PS) in this study were from 96.74 ± 3.15 % to 108.25 ± 6.83 % (Table S3), significantly outperforming the recovery rates for PP-MNPs (15.6 %–31.6 %) reported in a similar study [14]. This improvement can be attributed to the application of CPE, which excels in efficiently concentrating MNPs from large-volume solutions, significantly reducing particle loss and thereby maximizing recovery efficiency [21,22]. Specially, MNPs typically exhibit pronounced hydrophobic surface characteristics, which enable strong hydrophobic interactions with the micellar cores formed by nonionic surfactants near the cloud point temperature. This selective partitioning into the surfactant-rich phase substantially enhances the extraction efficiency. Second, CEP induces a pronounced phase separation upon reaching the cloud point, concentrating MNPs into a reduced-volume surfactant phase while effectively excluding the majority of matrix components into the aqueous phase. This is consistent with the relatively low matrix effect observed in this study (Table S3). Third, the tunable properties of the surfactant system allow the method

to efficiently capture a wide range of MNPs differing in size, surface chemistry, and polymer composition through the modulation of factors such as temperature, pH, and ionic strength. Together, these attributes confer a robust and highly adaptable extraction performance, positioning CEP as a powerful preconcentration strategy for MNP quantification in complex matrices.

For PAEs, procedural blank concentrations ranged from non-detectable (ND) levels to 24.83 ng/L, while the recovery rates for DEHP-d4 and DHP-d4 were 97.78 ± 13.72 % and 94.04 ± 13.81 %, respectively. These results align well with established methodologies for PAE analysis in various aquatic matrices, such as surface water and drinking water [25]. Collectively, the background levels for both MNPs and PAEs in this study are consistent with values reported in the previous reports, and the high recovery rates further validate the reliability and precision of our analytical methods for detecting and quantifying MNPs and PAEs.

3.2. Prevalence of MPs and NPs in medical infusion

MPs and NPs were detected across all analyzed infusion bag samples (Table 1). PP-MPs were found in all infusions, showing a 100 % detection frequency (DF), with concentrations ranging from 0.22 to 66.57 μg/L (median: 12.70 μg/L; mean ± SD: 20.05 ± 19.05 μg/L). Additionally, PE-MPs appeared in 88.89 % of all infusions, with concentrations from ND to 181.76 μg/L (median: 8.53 μg/L; mean ± SD: 29.89 ± 51.04 μg/L). PS-MPs were less prevalent, detected in 72.22 % of all infusions, with a lower median concentration (0.66 μg/L) and a narrower range (ND–15.68 μg/L). In the glucose infusions, all PE-MPs, PP-MPs and PS-MPs showed 100 % detection, with exhibiting a median concentration of 32.27, 13.43, and 5.45 μg/L, respectively. For NPs, PP-NPs exhibited a 100 % in both glucose and saline infusions, ranging from 7.56 to 242.39 μg/L in the glucose infusions (median: 55.00 μg/L, mean ± SD: 84.82 ± 94.71 μg/L) and 4.25–224.26 μg/L in saline infusions (median: 43.55 μg/L, mean ± SD: 89.56 ± 84.69 μg/L). PS-NPs were also ubiquitous, detected in 94.44 % of all infusions, with a notably higher median concentration in glucose infusions (53.85 μg/L) compared to saline infusions (16.98 μg/L).

When considering total MNPs, all infusion bag samples contained detectable MNPs, with concentrations ranging from 48.97 to 628.99 μg/L. The median MNP concentration in glucose infusions (430.68 μg/L) was slightly higher than in saline infusions (338.69 μg/L), with overall means of 381.00 ± 201.26 μg/L and 335.65 ± 118.91 μg/L, respectively. Notably, NPs comprised the majority of the total plastic burden regarding median concentration, with PE-NPs, PP-NPs and PS-NPs significantly contributing to the observed contamination levels. Moreover, the MNP content within different batches of infusion solutions remained stable, with no significant differences observed (Figure S2). The results of the mass concentration were further cross-validated by particle count measurements. NTA results indicated the presence of nanoparticles in the infusion solutions within the concentration range of $4.3 \times 10^6 - 1.2 \times 10^8$ (Figure S3 and S4), which indirectly supports the presence of a substantial amount of nanoparticles in the solutions. Nevertheless, after storage under simulated real-world conditions, the degree of plastic packaging aging was minimal by 2D-COS analysis (Figure S5, S6, and S7). Furthermore, neither the mass concentration nor the particle number concentration showed significant changes before and after storage (Figure S3 and S8).

Notably, the NTA results revealed distinct differences in NP distribution patterns among various infusion bag samples, underscoring the complexity of NP contamination in clinical fluids. Three typical scenarios were observed. (1) In certain samples, strong NP signals in the 0–50 nm range were consistently detected in both the original and simulated storage batches (e.g., saline 3 and simulated saline 3; glucose 3 and simulated glucose 3), suggesting the presence of ultrafine, non-dissolvable particles. These are likely introduced during the manufacturing process or released from the plastic infusion bags themselves. (2) In other cases, NP signals were observed in the original batch but disappeared after simulated storage (e.g., glucose 2), which may indicate the presence of soluble nano-sized colloidal particles that were gradually dissolved over time during the storage simulation. (3) Conversely, some samples showed an absence of NPs in the original batch but exhibited strong signals post-simulation (e.g., saline 2). This suggests a potential delayed release of NPs from the packaging materials. While no statistically significant increase in the total concentration of MNPs was observed across all samples, these sporadic enhancements in the nanoscale range highlight the necessity for more comprehensive and condition-specific assessments of NP release. These findings call for continued vigilance in the monitoring of infusion product safety, particularly concerning their potential for NP contamination.

There is a limited amount of directly comparable data available. Currently, Zhu et al. [16] have investigated MPs in PP, PE, and

Table 1
Prevalence of MNPs in infusion (μg/L; n = 6–12). ND: No detection.

Prevalence of MNPs in Medical Infusion					
	MNPs	**DF (%)**	**Range**	**Median**	**Mean ± SD**
All infusion	PE-MPs	88.89	ND – 181.76	8.53	29.89 ± 51.04
	PP-MPs	100	0.22 – 66.57	12.70	20.05 ± 19.05
	PS-MPs	72.22	ND – 15.68	0.66	2.82 ± 4.84
	MPs	100	2.96 – 225.03	25.04	52.76 ± 64.30
	PE-NPs	100	13.24 – 568.77	87.54	143.87 ± 143.46
	PP-NPs	100	4.25 – 242.39	43.55	87.98 ± 85.36
	PS-NPs	94.44	ND – 234.24	29.09	62.16 ± 72.36
	NPs	100	46.01 – 617.52	314.45	298.00 ± 165.12
	PE-MNPs	100	15.52–570.45	125.27	177.75 ± 154.61
	PP-MNPs	100	9.71 – 278.12	54.76	108.03 ± 95.85
	PS-MNPs	94.44	ND – 238.05	30.45	64.98 ± 74.05
	MNPs	100	48.97 – 628.99	346.79	350.77 ± 183.23
Glucose	PE-MPs	100	10.51 – 181.76	32.27	68.85 ± 74.80
	PP-MPs	100	0.22 – 66.57	13.43	21.94 ± 26.01
	PS-MPs	100	0.01 – 15.68	5.45	7.11 ± 6.63
	MPs	100	14.87 – 225.03	53.98	97.90 ± 95.39
	PE-NPs	100	51.58 – 176.44	116.76	119.41 ± 52.02
	PP-NPs	100	7.56 – 242.39	55.00	84.82 ± 94.71
	PS-NPs	100	9.70 – 170.10	53.85	78.88 ± 69.09
	NPs	100	113.16 – 453.03	316.99	283.10 ± 140.15
	PE-MNPs	100	62.09 – 358.20	149.02	188.26 ± 122.41
	PP-MNPs	100	9.71 – 278.12	88.77	106.76 ± 112.11
	PS-MNPs	100	9.71 – 174.75	65.00	85.99 ± 71.28
	MNPs	100	130.23 – 596.39	430.68	381.00 ± 201.26
Saline	PE-MPs	83.33	ND –40.42	2.04	10.40 ± 15.48
	PP-MPs	100	0.69 – 57.39	12.69	19.11 ± 15.83
	PS-MPs	58.33	ND – 3.81	0.35	0.68 ± 1.10
	MPs	100	2.96 – 77.11	19.50	30.20 ± 24.25
	PE-NPs	100	13.24 – 568.77	75.09	162.09 ± 172.96
	PP-NPs	100	4.25 – 224.26	43.55	89.56 ± 84.69
	PS-NPs	91.67	ND – 234.24	16.98	53.80 ± 75.46
	NPs	100	46.01 – 617.52	314.32	305.45 ± 181.74
	PE-MNPs	100	15.52 – 570.45	95.80	172.50 ± 173.32
	PP-MNPs	100	17.00 – 236.20	54.76	108.67 ± 92.11
	PS-MNPs	91.67	ND – 238.04	17.26	54.47 ± 76.18
	MNPs	100	48.97 – 628.99	338.69	335.65 ± 180.91

glass-bottled infusions. They found only a few larger-sized MPs (4–148 μm) in PP and PE packaging, which may be attributed to the Raman spectroscopy method they used. Increasingly, evidence suggests that both traditional Raman and infrared spectroscopy may struggle with detecting smaller particles, particularly those at the nanoscale level [17, 18]. More recently, Huang et al. [10] identified MPs (1–62 μm) with concentrations reaching as high as 7500 particles per liter, by combining surface-enhanced Raman spectroscopy and scanning electron microscopy. Wang et al. [14] employed Py-GC/MS to study MNPs (PP and PE) in injectable solutions, finding NPs content ranging from 1 to 40 μg/L, which is partially consistent with our findings. In addition to the contamination by PE plastics in PP packaging infusion, we further identified the presence of PS plastic pollution. Therefore, our study reinforces the widespread occurrence of MNPs with varying properties in infusion solutions, including glucose and saline. With advances in separation and detection technologies, a broader range of MNPs is likely to be discovered, raising concerns regarding their potential environmental and health implications.

3.3. Distribution patterns of MPs and NPs in medical infusion

We further examined the distribution of MNPs in infusion solutions from multiple angles, including infusion type, plastic material, and particle size. PLS-DA analysis showed that MNPs, MPs, and NPs in glucose and saline solutions cluster together without clear separation, according to their respective statistical values, especially with a maximum $Q^2$of just 0.39 (Figs. 3a to 3b). Moreover, statistical comparisons revealed no significant differences in the concentrations of MNPs, MPs, and NPs between glucose and saline solutions (Figs. 3d to 3f), underscoring that both types of infusions contain similar levels of MNPs, with no marked variation in their concentrations. This suggests that the two commonly used infusion solutions in our study both contain MNPs at comparable concentrations.

From a plastic material perspective, there were no notable differences in the concentrations of PP-MNPs and PS-MNPs (Fig. 4a). However, PE-MNPs and PE-NPs showed significantly higher levels than PS-MNPs and PS-NPs (Figs. 4a and 4c). Additionally, both PE-MPs and PP-MPs were markedly higher than PS-MPs (Fig. 4b). However, PP-MPs exhibited substantially higher concentrations than PS-MPs (Fig. 4b), indicating that larger exogenous particles are relatively scarce, while smaller particles, which are more challenging to control, are more abundant. These smaller particles are likely to be released from the packaging material itself, contributing to the overall contamination. In terms of particle size, regardless of the material (PE, PP, PS, or their combination), NPs were present in significantly higher concentrations than MPs in both infusion bag samples (Figs. 4d to 4g). This further highlights the prevalence of NPs as the primary contaminants in commonly used infusion solutions, raising serious concerns about the potential health risks associated with their widespread presence. These findings emphasize the need for greater attention to the sources, distribution, and potential health impacts of MNPs contamination in medical and pharmaceutical applications.

MNPs, owing to their small particle size, have the capacity to infiltrate the systemic circulation and exhibit a remarkable potential to cross

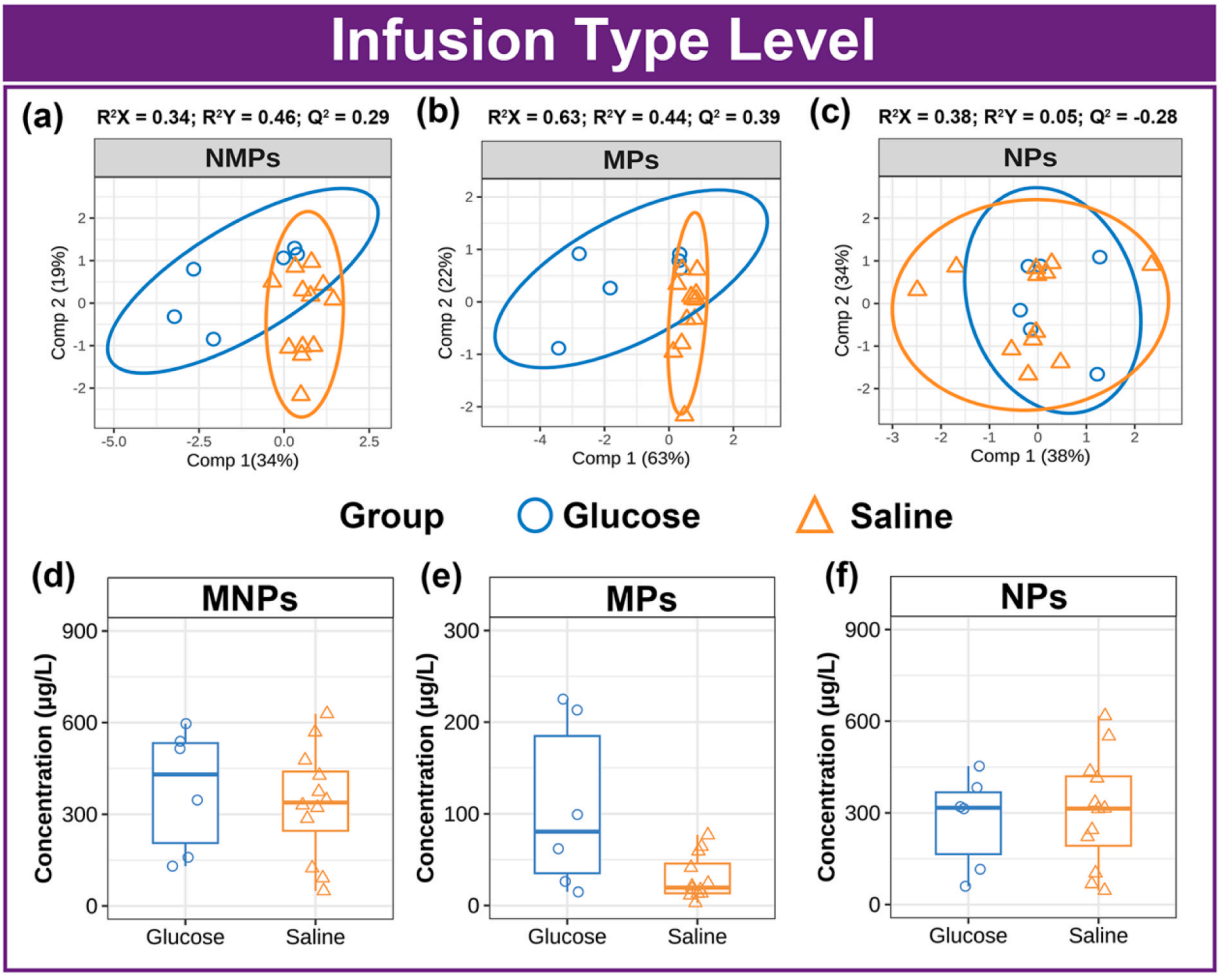

Fig. 3. Distribution patterns of MPs and NPs in different types of infusion solutions (n = 6 for glucose; n = 12 for saline). (a-b) PLS-DA of MNPs, MPs, and NPs in glucose and saline infusions. (d-f) The concentrations of MNPs, MPs, and NPs in glucose and saline infusions.

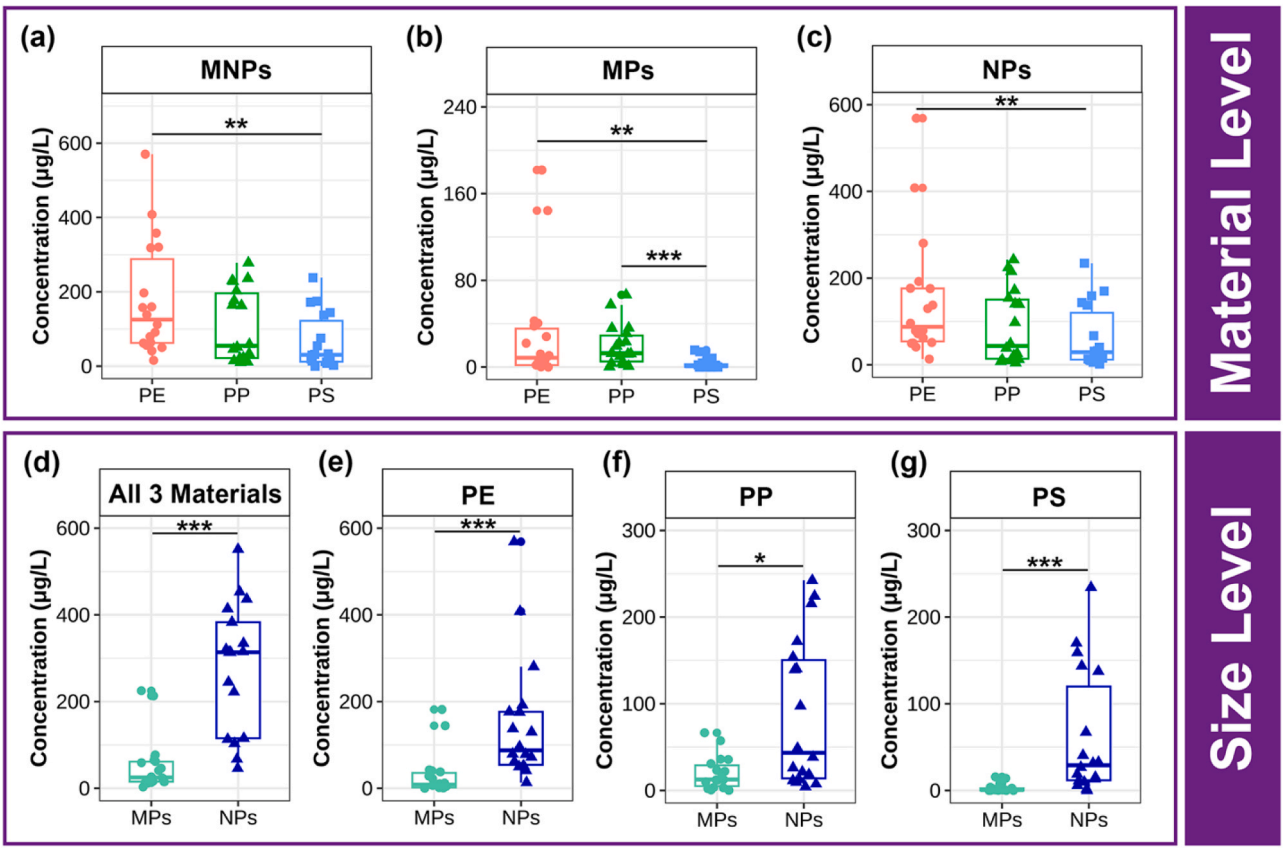

Fig. 4. Distribution patterns of MPs and NPs in infusion solutions from the perspectives of material and particle size (n = 18). (a-c) MNPs, MPs and NPs in infusion solutions from the perspectives of material. (d-g) MPs and NPs in infusion solutions from the perspectives of size. *, $P < 0.05$; **, $P < 0.01$; ***, $P < 0.001$.

biological barriers such as the blood-brain and blood-testis barriers, which has garnered significant attention [7]. It is well-established that the inner diameter of the smallest human capillaries is less than 20 μm [38-40], meaning that MNPs with sizes smaller than this threshold can migrate within the circulatory system. Upon reaching the liver, MNPs can directly disrupt critical metabolic functions, including lipid, amino acid, and energy metabolism [41,42]. Furthermore, studies indicate that nonbiodegradable particles larger than 5.5 nm can accumulate in hepatic Kupffer cells over extended periods [43], potentially triggering immune responses and inflammation, which may serve as a crucial mechanism for liver toxicity induced by MNPs [44]. Of particular concern, smaller NPs are capable of directly penetrating biological barriers, leading to other potential damage [45,46]. Therefore, these findings suggest a heightened potential for more severe and widespread health impacts, reinforcing the need for greater attention to the implications of MNPs contamination in medical treatments.

3.4. *Quantification and analysis of PAEs in medical infusion*

Among the ten PAEs analyzed, five PAEs, including DBP, DEP, DEHP, DIBP, and DMP, were detected in all infusion bag samples with a 100 % DF (Table 2), underscoring their widespread presence in the infusions. The total concentrations of these PAEs exhibited a considerable range, spanning from 65.71 to 2482.46 ng/L. Notably, DBP, DMP, and DIBP emerged as the top three contributors to the overall PAE concentration, accounting for the majority of the detected levels and emphasizing their significant prevalence in the infusion solutions. No significant difference in the distribution of PAEs was observed between glucose and saline solutions (Fig. 5a). Saline infusions consistently exhibited higher median concentrations of PAEs compared to glucose infusions (Fig. 5b), with the sum of all PAEs ranging from 220.48 to 1042.70 ng/L in glucose infusions and from 65.71 to 2482.46 ng/L in saline infusions, reflecting a higher overall contamination burden in saline infusions.

For the individual PAEs (Fig. 5c), DBP is the most abundant, with concentrations ranging from 104.69 to 435.52 ng/L in glucose infusions (median: 247.43 ng/L) and from 36.54 to 771.69 ng/L in saline infusions (median: 279.16 ng/L), making it the dominant PAE in both solutions, particularly in saline infusions, where its levels are notably elevated. DBzP and DHP exhibits relatively lower concentrations in all infusions. Other PAEs, such as DEHP and DIBP, demonstrate fairly consistent concentrations across both solutions, with DIBP showing higher levels in saline infusions (median: 75.32 ng/L). DMP, which exhibits considerable variability, especially in saline infusions, where its range spans from 1.87 to 1394.34 ng/L (mean of 391.12 ± 487.24 ng/L), contributing significantly to the overall higher mean concentration observed in saline infusions. This data highlights the complex distribution and varying prevalence of PAEs, with saline infusions consistently displaying higher levels of contamination, which warrants further investigation into the sources and environmental implications of these compounds.

Our study provides evidence of the presence of various types and concentrations of PAEs in PP packaging bags, marking a significant divergence from previous research, which predominantly focused on PVC-based infusion packaging and reported elevated levels of DEHP in PVC products [47,48]. DEHP is widely recognized for its role in enhancing the flexibility, durability, and processability of PVC materials. However, DEHP is also known to exhibit considerable reproductive toxicity, leading to strict regulatory oversight on the use of toxic PAEs in medical devices by numerous governmental agencies [49]. In contrast to PVC, PP is inherently more flexible than many other polymers, and its physical properties can be tailored through copolymerization or blending with other materials, obviating the need for plasticizers such as

Table 2
Prevalence of PAEs in infusions (ng/L, n = 6–12). ND: No detection.

Prevalence of PAEs in Medical Infusion					
	PAE	DF (%)	Range	Median	Mean ± SD
All infusion	BMPP	56 %	ND – 52.94	1.79	14.86 ± 18.94
	DAmP	33.33 %	ND – 19.44	ND	2.82 ± 5.49
	DBP	100 %	36.53 – 771.69	258.72	306.63 ± 224.41
	DBzP	27.78 %	ND – 17.40	ND	1.41 ± 4.12
	DEP	100 %	4.64 – 457.43	38.20	91.91 ± 125.88
	DEHP	100 %	1.00 – 138.03	31.74	48.03 ± 49.15
	DHP	5.56 %	ND – 10.69	ND	0.59 ± 2.52
	DIBP	100 %	12.48 – 241.41	60.16	99.90 ± 83.13
	DMP	100 %	1.87 – 1394.34	105.99	282.78 ± 423.85
	DPhP	33.33 %	ND–210.43	ND	25.40 ± 53.57
	SumPAEs	100 %	65.71 – 2482.46	757.56	874.34 ± 704.66
Glucose	BMPP	50 %	ND – 52.94	18.80	22.51 ± 25.13
	DAmP	50 %	ND – 19.44	0.67	5.46 ± 8.30
	DBP	100 %	104.69 – 435.52	247.43	263.94 ± 145.44
	DBzP	33.33 %	ND – 1.54	ND	0.35 ± 0.62
	DEP	100 %	11.69 – 193.63	37.60	62.71 ± 69.48
	DEHP	100 %	2.20 – 125.51	39.10	52.85 ± 53.92
	DHP	ND	ND	ND	ND
	DIBP	100 %	21.32 – 133.38	60.07	69.98 ± 47.68
	DMP	100 %	6.92 – 150.28	50.44	66.10 ± 63.25
	DPhP	50 %	ND – 210.43	36.16	62.64 ± 83.23
	SumPAEs	100 %	220.48 – 1042.70	505.26	606.53 ± 326.19
Saline	BMPP	58.00 %	ND – 43.38	1.79	11.04 ± 14.83
	DAmP	25.00 %	ND – 8.59	ND	1.51 ± 3.09
	DBP	100 %	36.54 – 771.69	279.16	327.98 ± 258.31
	DBzP	25 %	ND – 17.40	ND	1.94 ± 5.01
	DEP	100 %	4.64 – 457.44	40.76	106.51 ± 146.96
	DEHP	100 %	1.00 – 138.03	28.85	45.61 ± 48.92
	DHP	8.33 %	ND – 10.69	ND	0.89 ± 3.08
	DIBP	100 %	12.48 – 241.41	75.23	114.86 ± 96.41
	DMP	100 %	1.87 – 1394.34	150.79	391.12 ± 487.24
	DPhP	25 %	ND – 30.82	ND	6.78 ± 12.35
	SumPAEs	100 %	65.71 – 2482.46	1043.63	1008.24 ± 812.61

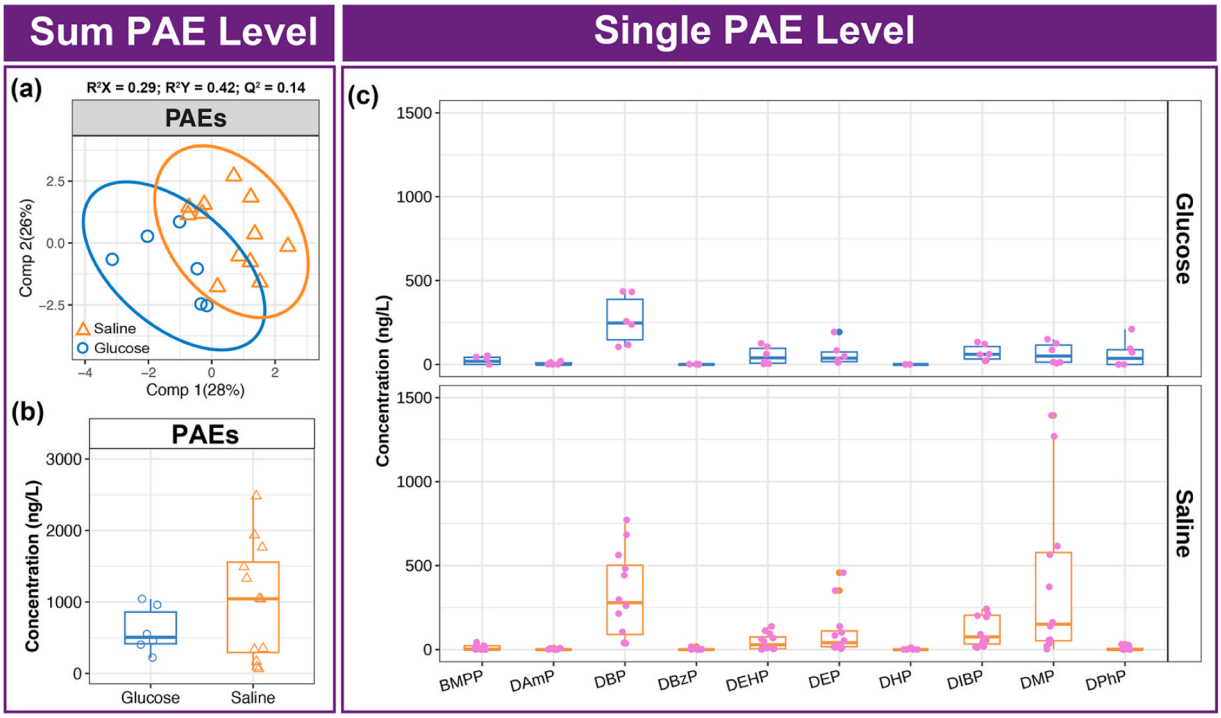

Fig. 5. Distribution patterns of ten PAEs in infusion solutions. (a) PLS-DA of PAEs (n = 6 for glucose; n = 12 for saline). (b) The sum PAE concentration (n = 6 for glucose; n = 12 for saline). (c) The single PAE concentration (n = 18).

PAEs [50]. Nevertheless, prior research has demonstrated that PP-based medical packaging can also release PAEs [51]. Consequently, the PAEs identified in the infusion solutions of this study may stem either from endogenous release from the PP material itself or from exogenous contamination introduced during the production process, as PAEs are widely pervasive in various environmental media [52]. More troublingly, similar to DEHP, the high concentrations of DBP, DMP, and DIBP found in our study are of particular concern, as they are potent endocrine disruptors associated with a broad range of health risks, particularly during critical periods of development, such as fetal development and sperm production [53]. In addition to their reproductive toxicity, these chemicals have been linked to a range of neurodevelopmental and behavioral disorders and potential cancer risks [54, 55]. Although the levels of PAEs in the infusion solutions are below the European Food Safety Authority's established Tolerable Daily Intake limit of 50 μg/kg body weight [56], continuous monitoring of the trends and potential toxicity of these contaminants in infusion solutions is still necessary.

3.5. Interrelationships among MPs, NPs, and PAEs

We also investigated the intrinsic relationships between plastic particles (MPs, NPs, and MNPs) and PAEs in infusions using Mantel and Spearman correlation tests (Fig. 6, and Table S5). Our results revealed significant positive correlations between PP-NPs and PP-MNPs ($r = 0.97$, $p < 0.001$), PE-NPs and PE-MNPs ($r = 0.98$, $p < 0.001$), PS-NPs and PS-MNPs ($r = 1.00$, $p < 0.001$), as well as between NPs and MNPs ($r = 0.92$, $p < 0.001$) concentrations. These correlations underscore the dominant role of NPs in the overall concentration of MNPs in the infusion solutions. More importantly, a significant positive correlation was observed between individual PAE and MNPs. Specifically, DAmP exhibited notable positive correlations with PS-MPs ($r = 0.56$, $p < 0.05$). Similarly, DEHP demonstrated significant positive correlations with PP-NPs ($r = 0.38$, $p < 0.01$). These findings preliminarily highlight a strong synergistic relationship between the release of MNPs and plastic additives in common infusion solutions. This suggests an increased likelihood of concurrent exposure to both MNPs and toxic PAEs, which may exacerbate potential health risks.

3.6. Evaluation of cardiovascular cytotoxicity induced by Co-exposure to NPs and PAEs

To further investigate the health risks associated with the combined exposure to MNPs and PAEs, we utilized HUVECs as an in vitro model. PS-NPs and DEHP were chosen as representative compounds to examine the effects of mixed exposure on cell viability and the expression of genes linked to inflammation, lipid metabolism, and apoptosis.

In terms of cell viability, exposure to PS-NPs alone significantly inhibited cell viability starting at a concentration of 25 μg/mL, with a dose-dependent reduction observed as the exposure concentration increased (Figure S9). Similarly, exposure to DEHP alone resulted in a significant decrease in cell viability beginning at 70 ng/mL, with further suppression observed at higher concentrations (Figure S9). Notably, combined exposure to PS-NPs and DEHP caused a more pronounced reduction in cell viability compared to individual exposures (Fig. 7a), suggesting a potential synergistic enhancement of toxicity. At the gene expression level, combined exposure to PS-NPs and DEHP further significantly downregulated the expression of *Caspase-3* and *ITGA4*, while significantly upregulating *PPARγ* expression (Fig. 7b). These findings provide compelling evidence of the synergistic toxic effects of PS-NPs and DEHP, which may be mediated through alterations in key signaling pathways associated with apoptosis, inflammatory response, and lipid metabolism [29-31].

The synergistic effects of plastic particles and other contaminants, such as plasticizers, represent a critical yet often overlooked issue in plastic pollution. Emerging evidence suggests that the co-exposure of MNPs and PAEs could exacerbate toxicological outcomes compared to individual exposures [23,57]. For example, MNPs can increase the

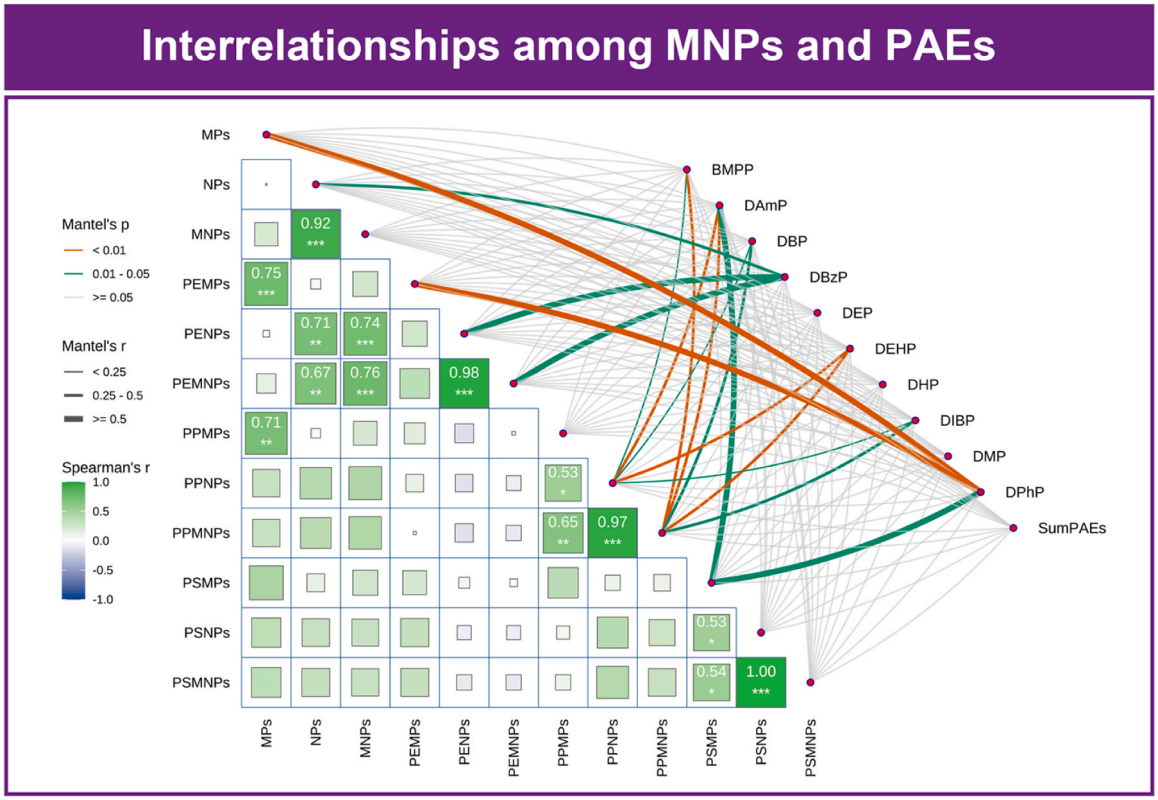

Fig. 6. Interrelationships among MPs, NPs, and PAEs in infusions (n = 18). *, $P < 0.05$; **, $P < 0.01$; ***, $P < 0.001$.

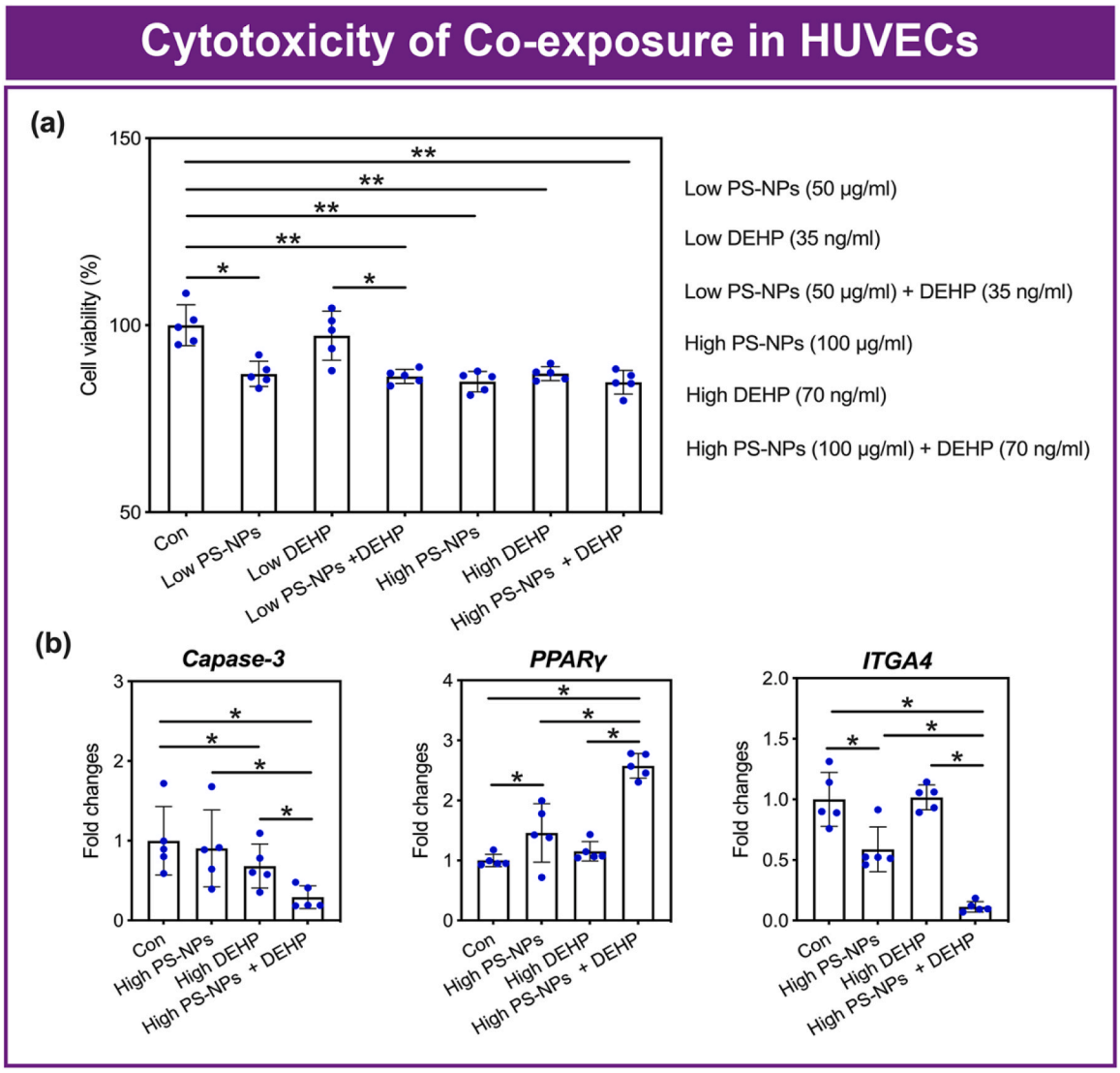

Fig. 7. Cytotoxicity of co-exposure to PS-NPs and DEHP in HUVECs (n = 5). (a) Cell viability; (b) Gene expression levels. *, $P < 0.05$; **, $P < 0.01$; ***, $P < 0.001$.

uptake and retention of PAEs in biological tissues, potentially enhancing the toxic effects of MNP exposure [58]. This interaction may lead to amplified immune responses, increased inflammation, and potentially more severe endocrine disruption [24,59]. In alignment with previous studies, our findings show that co-exposure to PS-NPs and DEHP further suppressed cell viability and significantly interfered with key cellular processes, including apoptosis, inflammatory responses, and lipid metabolism. While direct evidence linking MNPs and phthalate esters PAEs in infusion solutions to human health risks is still scarce, the risk of synergistic effects from co-exposure in infusion solutions may be even more pronounced. Infusion-based exposure is more direct, as both MNPs and PAEs are readily transported into the systemic circulation and distributed throughout the body. The patients requiring infusions are often immunocompromised or have underlying health conditions, making them particularly vulnerable to the compounded toxicity of MNPs and PAEs. The potential for amplified toxic effects, especially in long-term infusion therapy, underscores the urgent need to reassess the safety of medical products containing such contaminants. In addition, future research should further investigate the mechanistic pathways underlying the co-exposure toxicity of nanoparticles and PAEs in infusion solutions, which will be critical for identifying potential detoxification strategies. It is also essential to consider the role of particle surface properties in modulating toxicity and to collect more human-relevant data to enable a comprehensive assessment of potential health risks.

3.7. Limitation

Our study is the first to demonstrate that infusion therapy, as a distinct exposure route, can simultaneously introduce PE, PP and PS-MNPs along with toxic PAEs directly into the bloodstream, and induce serious cytotoxicity. This intravascular exposure pathway bypasses primary biological barriers, potentially amplifying health risks beyond those associated with conventional environmental exposures.

Nevertheless, our study also presented several limitations.In terms of the research content: (1) We focused exclusively on PE, PP and PS, due to their widespread occurrence and significant toxicity [4,60]. However, to gain a more comprehensive understanding of MNPs in medical infusion, future research should explore other common materials, such as PVC and PET, which may also prevalent in infusion products. Furthermore, the release of other potential contaminants, such as phosphorus-based flame retardants, antimicrobial agents, and antioxidants, should be considered, in addition to the PAEs analyzed in this study. (2) The study analyzed infusion bag samples from nine different brands, which reflects a limited market sample due to the exclusion of duplicates and the challenge of tracking different product batches. Given

the wide array of brands in the market, future research should increase the sample size to include more brands and assess whether similar trends in MNPs and PAE concentrations are observed across a broader range of products. (3) This study focused on hospitals in three major Chinese cities, which may not fully represent global trends. While valuable data on domestic markets was obtained, future studies should incorporate samples from a variety of countries to assess regional and international differences in the release patterns of MNPs and PAEs. Cross-national studies will provide a more comprehensive understanding of the global prevalence and potential health risks posed by these contaminants. (4) We predominantly explored MNP and PAEs release from PP-based infusion bags. However, other materials, such as PE and PVC, may be used in medical infusion systems and release MNPs and additives at different rates. Future research should investigate whether similar contamination trends occur across various plastic materials used in infusion bags and other components of the infusion system. (5) We primarily focused on glucose and saline infusion solutions, which represent common clinical fluids. However, future research should expand the scope to investigate a wider range of infusion types, such as amino acid solutions, lipid emulsions, and other specialized infusions, to evaluate whether they also contribute to plastic contamination and whether their characteristics influence the release of MNPs and PAEs. (6) In addition to infusion bags, other components of the infusion system, including infusion tubes and syringes, may also contribute to the introduction of MNPs. However, due to time and resource limitations, it is not feasible to conduct a comprehensive analysis of all components within the scope of a single study. Our investigation of MNPs in infusion bags serves as the starting point for the system, providing a foundation for future research on the release of MNPs from other parts of the infusion system, along with the associated methodological and technical support. (7) The infusions used in this study were from the hospitals with strictly controlled storage conditions to minimize environmental variables. However, future research should consider how variations in temperature, humidity, light exposure, and storage duration may influence the release of MNPs and additives [61,62]. Incorporating these factors will provide a more realistic view of how MNP behave under varying environmental conditions, and multivariate regression analysis could be employed to identify key factors that influence these release patterns.

The high recovery efficiencies observed in this study highlight the robustness and effectiveness of the method. However, further optimization and enhancement of the technology are necessary in the following areas. (1) The analytical methods should be validated for their applicability to other types of particles, to ensure that the separation and detection capabilities are universally effective across various materials. (2) Although efforts were employed to reduce nonionic surfactant interference in CPE, residual surfactants could still impact the quantification of MNPs. Future research should address this potential interference and refine the methodology to minimize such effects. (3) Future work should focus on optimizing the CPE and Py-TD-GC/MS platforms to improve the efficiency of MNP extraction and detection. Enhancing the throughput and detection sensitivity of these techniques will be crucial for high-volume applications in MNP analysis. (4) The study utilized laboratory-grade standard plastics for quantifying MNPs in infusion solutions, which may not fully reflect the characteristics of plastics used in clinical settings, where degradation and aging may occur. Although stringent storage regulations minimize plastic aging in medical infusions, future research should investigate the potential impact of storage deviations, such as increased temperatures or prolonged storage, which could accelerate plastic degradation and lead to higher levels of MNP release.

3.8. Prospective approaches for mitigating risks

Given the unprecedented level of internal contamination, this issue demands urgent attention, necessitating not only heightened awareness but also the implementation of stringent regulatory policies and the development of safer material alternatives to mitigate potential health risks and safeguard intravenous medical treatments. Regulatory frameworks must be reinforced to restrict the use of hazardous PAEs in medical products and packaging. While certain regions have imposed bans or limitations on high-risk PAEs, such as DEHP in medical devices, expanding these regulations to encompass other toxic plasticizers, including DBP and DIBP, would further reduce exposure risks. Material innovation is imperative to decrease reliance on conventional plasticizers. Beyond prevention, enhancing monitoring capabilities is crucial. Implementing real-time monitoring systems could provide continuous quality control, ensuring contamination levels remain within safe limits. Finally, patient safety protocols must be adapted to mitigate the risks of MNP and PAE exposure. This includes transitioning to safer packaging and infusion systems free from harmful plasticizers, minimizing the use of plastic-based medical devices when alternatives are available, and incorporating risk assessment strategies into medical guidelines. A collaborative effort among policymakers, healthcare providers, and material scientists will be essential to developing sustainable, low-toxicity solutions that prioritize both medical efficacy and long-term patient safety.

4. Conclusion

In summary, we present a highly efficient method for the separation and quantification of MNPs utilizing CPE combined with Py-TD-GC/MS, which reveals the presence of various MNPs, including PE-MPs, PE-NPs, PP-MPs, PP-NPs, PS-MPs, and PS-NPs, in commonly used PP-based glucose and saline infusions. Notably, NPs were found to be significantly more prevalent than MPs. Additionally, we identified widespread contamination by ten PAEs in these infusions, with DBP, DMP, and DIBP being the most abundant. A concerning positive correlation was observed between the concentrations of MNPs and PAEs, suggesting that intravenous exposure through infusion therapy may result in concurrent exposure to both MNPs and PAEs. Of particular significance, co-exposure to PS-NPs and DEHP not only further suppressed cell viability but also disrupted key cellular processes, including apoptosis, inflammation, and lipid metabolism, highlighting the potential for synergistic toxic effects. These findings underscore the critical need for continued research into this novel exposure pathway and stress the importance of developing effective mitigation strategies to minimize the health risks associated with MNPs and hazardous additives in medical applications.

Author contributions

Y.F.D. designed the study and supervised all parts of the project. X.Z., R.Q.S., P.X. performed animal experiments. X.Z., R.Q.S., P.X. performed data analyses. Y.F.D, J X.Z., R.Q.S., P.X., and H.I.T, drafted the initial and revised versions of the paper. Y.F.D. provided funding support. All authors approved the final version of the paper.

CRediT authorship contribution statement

Peng Xia: Investigation. **Ruqin Shen:** Methodology, Investigation, Data curation. **Hongli Tan:** Writing – original draft. **Xue Zhang:** Writing – original draft, Investigation, Data curation. **Yongfeng Deng:** Writing – original draft, Supervision, Funding acquisition, Conceptualization.

Declaration of Competing Interest

The authors declare that they have no known competing financial interests or personal relationships that could have appeared to influence the work reported in this paper.

Acknowledgments

This work was financially supported by the Natural Science Foundation of China (No. 22276073), the Jiangsu Province Young Science and Technology Talent Support Program (No. JSTJ-2024–095), Nanjing Outstanding Young and Middle-Aged Talent Program (No. Q(2024) 023), the Guangdong Basic and Applied Basic Research Foundation (No. 2022A1515010722), the Joint Fund of Departments and Schools (No. 2242024K40045), the Start-up Research Fund (No. RF1028623238), and the Zhishan Young Scholars Fund (No. 2242024RCB0027) of Southeast University by the Fundamental Research Funds for the Central Universities.

Appendix A. Supporting information

Supplementary data associated with this article can be found in the online version at doi:10.1016/j.jhazmat.2025.139614.

Data availability

Data will be made available on request.

References

[1] Guan, Q., Jiang, J., Huang, Y., Wang, Q., Liu, Z., Ma, X., Yang, X., Li, Y., Wang, S., Cui, W., 2023. The landscape of micron-scale particles including microplastics in human enclosed body fluids. J Hazard Mater 442, 130138. https://doi.org/10.1016/j.jhazmat.2022.130138.

[2] Zhu, L., Kang, Y., Ma, M., Wu, Z., Zhang, L., Hu, R., Xu, Q., Zhu, J., Gu, X., An, L., 2024. Tissue accumulation of microplastics and potential health risks in human. Sci Total Environ 915, 170004. https://doi.org/10.1016/j.scitotenv.2024.170004.

[3] Marfella, R., Prattichizzo, F., Sardu, C., Fulgenzi, G., Graciotti, L., Spadoni, T., D'Onofrio, N., Scisciola, L., La Grotta, R., Frigé, C., 2024. Microplastics and nanoplastics in atheromas and cardiovascular events. N Engl J Med 390 (10), 900–910. https://doi.org/10.1056/NEJMoa2309822.

[4] Yan, Z., Liu, Y., Zhang, T., Zhang, F., Ren, H., Zhang, Y., 2021. Analysis of microplastics in human feces reveals a correlation between fecal microplastics and inflammatory bowel disease status. Environ Sci Technol 56 (1), 414–421. https://doi.org/10.1021/acs.est.1c03924.

[5] Deng, X., Gui, Y., Zhao, L., 2025. The micro (nano) plastics perspective: exploring cancer development and therapy. Mol Cancer 24 (1), 30. https://doi.org/10.1186/s12943-025-02230-z.

[6] Koelmans, A.A., Redondo-Hasselerharm, P.E., Nor, N.H.M., de Ruijter, V.N., Mintenig, S.M., Kooi, M., 2022. Risk assessment of microplastic particles. Nat Rev Mater 7 (2), 138–152. https://doi.org/10.1038/s41578-021-00411-y.

[7] Mitrano, D.M., Wick, P., Nowack, B., 2021. Placing nanoplastics in the context of global plastic pollution. Nat Nanotechnol 16 (5), 491–500. https://doi.org/10.1038/s41565-021-00888-2.

[8] Li, P., Liu, J., 2024. Micro (nano) plastics in the human body: sources, occurrences, fates, and health risks. Environ Sci Technol 58 (7), 3065–3078. https://doi.org/10.1021/acs.est.3c08902.

[9] Fang, C., Luo, Y., Naidu, R., 2023. Microplastics and nanoplastics analysis: options, imaging, advancements and challenges. TrAC Trends Anal Chem, 117158. https://doi.org/10.1016/j.trac.2023.117158.

[10] Huang, T., Liu, Y., Wang, L., Ruan, X., Ge, Q., Ma, M., Wang, W., You, W., Zhang, L., Valev, V.K., 2025. MPs entering human circulation through infusions: a significant pathway and health concern. Environ Health. https://doi.org/10.1021/envhealth.4c00210.

[11] Huang, H., Hou, J., Li, M., Wei, F., Liao, Y., Xi, B., 2025. Microplastics in the bloodstream can induce cerebral thrombosis by causing cell obstruction and lead to neurobehavioral abnormalities. Sci Adv 11 (4), eadr8243. https://doi.org/10.1126/sciadv.adr8243.

[12] Nihart, A.J., Garcia, M.A., El Hayek, E., Liu, R., Olewine, M., Kingston, J.D., Castillo, E.F., Gullapalli, R.R., Howard, T., Bleske, B., 2025. Bioaccumulation of microplastics in decedent human brains. Nat Med 1–6. https://doi.org/10.1016/j.nantod.2024.102466.

[13] Wright, S.L., Kelly, F.J., 2017. Plastic and human health: a micro issue? Environ Sci Technol 51 (12), 6634–6647. https://doi.org/10.1021/acs.est.7b00423.

[14] Wang, J., Xie, L.-G., Wu, X.-F., Zhao, Z.-G., Yang, H.-Y., Sun, H.-M., 2024. Identification and quantification of micro–nano-plastics in polypropylene-bottled injections. Heliyon 10 (15), e35101. https://doi.org/10.1016/j.heliyon.2024.e35101.

[15] Cui, T., Liu, K., Zhu, L., Wang, X., Dong, X., Jabeen, K., Zong, C., Wang, X., Wei, N., He, Y., 2024. Is intravenous infusion an unrecognized route for internal microplastic human exposure? A general assessment. J Hazard Mater 480, 135769. https://doi.org/10.1016/j.jhazmat.2024.135769.

[16] Zhu, L., Ma, M., Sun, X., Wu, Z., Yu, Y., Kang, Y., Liu, Z., Xu, Q., An, L., 2023. Microplastics entry into the blood by infusion therapy: few but a direct pathway. Environ Sci Technol Lett 11 (2), 67–72. https://doi.org/10.1021/acs.estlett.3c00905.

[17] Rauert, C., Charlton, N., Bagley, A., Dunlop, S.A., Symeonides, C., Thomas, K.V., 2025. Assessing the efficacy of Pyrolysis–Gas Chromatography–Mass spectrometry for nanoplastic and microplastic analysis in human blood. Environ Sci Technol 59 (4), 1984–1994. https://doi.org/10.1021/acs.est.4c12599.

[18] Schymanski, D., Oßmann, B.E., Benismail, N., Boukerma, K., Dallmann, G., Von der Esch, E., Fischer, D., Fischer, F., Gilliland, D., Glas, K., 2021. Analysis of microplastics in drinking water and other clean water samples with micro-Raman and micro-infrared spectroscopy: minimum requirements and best practice guidelines. Anal Bioanal Chem 413 (24), 5969–5994. https://doi.org/10.1007/s00216-021-03498-y.

[19] Xu, Y., Ou, Q., Jiao, M., Liu, G., Van Der Hoek, J.P., 2022. Identification and quantification of nanoplastics in surface water and groundwater by pyrolysis gas chromatography–mass spectrometry. Environ Sci Technol 56 (8), 4988–4997. https://doi.org/10.1021/acs.est.1c07377.

[20] Adhikari, S., Kelkar, V., Kumar, R., Halden, R.U., 2022. Methods and challenges in the detection of microplastics and nanoplastics: a mini-review. Polym Int 71 (5), 543–551. https://doi.org/10.1002/pi.6348.

[21] Zhou, X., Hao, L., Wang, H., Li, Y., Liu, J., 2018. Cloud-point extraction combined with thermal degradation for nanoplastic analysis using pyrolysis gas chromatography–mass spectrometry. Anal Chem 91 (3), 1785–1790. https://doi.org/10.1021/acs.analchem.8b04729.

[22] Li, Q., Lai, Y., Yu, S., Li, P., Zhou, X., Dong, L., Liu, X., Yao, Z., Liu, J., 2021. Sequential isolation of microplastics and nanoplastics in environmental waters by membrane filtration, followed by cloud-point extraction. Anal Chem 93 (10), 4559–4566. https://doi.org/10.1021/acs.analchem.0c04996.

[23] Deng, Y., Yan, Z., Shen, R., Huang, Y., Ren, H., Zhang, Y., 2021. Enhanced reproductive toxicities induced by phthalates contaminated microplastics in Male mice (*mus musculus*). J Hazard Mater 406, 124644. https://doi.org/10.1016/j.jhazmat.2020.124644.

[24] Deng, Y., Yan, Z., Shen, R., Wang, M., Huang, Y., Ren, H., Zhang, Y., Lemos, B., 2020. Microplastics release phthalate esters and cause aggravated adverse effects in the mouse gut. Environ Int 143, 105916. https://doi.org/10.1016/j.envint.2020.105916.

[25] Deng, H., Li, R., Yan, B., Li, B., Chen, Q., Hu, H., Xu, Y., Shi, H., 2021. PAEs and PBDEs in plastic fragments and wetland sediments in Yangtze estuary. J Hazard Mater 409, 124937. https://doi.org/10.1016/j.jhazmat.2020.124937.

[26] Rauert, C., Wang, X., Charlton, N., Lin, C.-Y., Tang, C., Zammit, I., Jayarathne, A., Symeonides, C., White, E., Christensen, M., 2024. Blueprint for the design, construction, and validation of a plastic and phthalate-minimised laboratory. J Hazard Mater 468, 133803. https://doi.org/10.1016/j.jhazmat.2024.133803.

[27] Domenech, J., Villacorta, A., Ferrer, J.F., Llorens-Chiralt, R., Marcos, R., Hernández, A., Catalán, J., 2024. In vitro cell-transforming potential of secondary polyethylene terephthalate and polylactic acid nanoplastics. J Hazard Mater 469, 134030. https://doi.org/10.1016/j.jhazmat.2024.134030.

[28] Wu, H., Liu, Q., Yang, N., Xu, S., 2023. Polystyrene-microplastics and DEHP co-exposure induced DNA damage, cell cycle arrest and necroptosis of ovarian granulosa cells in mice by promoting ROS production. Sci Total Environ 871, 161962. https://doi.org/10.1016/j.scitotenv.2023.161962.

[29] Ahmadian, M., Suh, J.M., Hah, N., Liddle, C., Atkins, A.R., Downes, M., Evans, R. M., 2013. PPARγ signaling and metabolism: the good, the bad and the future. Nat Med 19 (5), 557–566. https://doi.org/10.1038/nm.3159.

[30] Li, M., Ye, J., Xia, Y., Li, M., Li, G., Hu, X., Su, X., Wang, D., Zhao, X., Lu, F., 2022. METTL3 mediates chemoresistance by enhancing AML homing and engraftment via ITGA4. Leukemia 36 (11), 2586–2595. https://doi.org/10.1038/s41375-022-01696-w.

[31] Ponder, K.G., Boise, L.H., 2019. The prodomain of caspase-3 regulates its own removal and caspase activation. Cell Death Discov 5 (1), 56–65. https://doi.org/10.1038/s41420-019-0142-1.

[32] Furukawa, T., Sato, H., Kita, Y., Matsukawa, K., Yamaguchi, H., Ochiai, S., Siesler, H.W., Ozaki, Y., 2006. Molecular structure, crystallinity and morphology of polyethylene/polypropylene blends studied by Raman mapping, scanning electron microscopy, wide angle X-ray diffraction, and differential scanning calorimetry. Polym J 38 (11), 1127–1136. https://doi.org/10.1295/polymj.PJ2006056.

[33] Guo, X., Lin, Z., Wang, Y., He, Z., Wang, M., Jin, G., 2019. In-line monitoring the degradation of polypropylene under multiple extrusions based on Raman spectroscopy. Polymers 11 (10), 1698. https://doi.org/10.3390/polym11101698.

[34] Gupta, C., Kaushik, S., Jain, S., Dhanwani, I., Garg, S., Paul, A., Pant, P., Gupta, N., 2022. Bioaccumulation and toxicity of polystyrene nanoplastics on marine and terrestrial organisms with possible remediation strategies: a review. Environ Adv 8, 100227. https://doi.org/10.1016/j.envadv.2022.100227.

[35] Bartnick, R., Rodionov, A., Oster, S.D.J., Löder, M.G., Lehndorff, E., 2024. Plastic quantification and polyethylene overestimation in agricultural soil using Large-Volume pyrolysis and TD-GC-MS/MS. Environ Sci Technol 58 (29), 13047–13055. https://doi.org/10.1021/acs.est.3c10101.

[36] Zhu, L., Wu, Z., Dong, J., Zhao, S., Zhu, J., Wang, W., Ma, F., An, L., 2024. Unveiling Small-Sized plastic particles hidden behind Large-Sized ones in human excretion and their potential sources. Environ Sci Technol 58 (27), 11901–11911. https://doi.org/10.1021/acs.est.3c11054.

[37] Liu, Y., Han, J., Wang, Y., Li, A., Zhao, J., Su, Y., Shen, L., Xing, B., 2024. Suspected sources of microplastics and nanoplastics: contamination from experimental reagents and solvents. Water Res 249, 120925. https://doi.org/10.1016/j.watres.2023.120925.

[38] Bukhari, M., Hollis, S., Moore, T., Jayson, M., Herrick, A., 2000. Quantitation of microcirculatory abnormalities in patients with primary raynaud's phenomenon

and systemic sclerosis by video capillaroscopy. Rheumatology 39 (5), 506–512. https://doi.org/10.1093/rheumatology/39.5.506.
[39] Graceffa, D., Amorosi, B., Maiani, E., Bonifati, C., Chimenti, M.S., Perricone, R., Di Carlo, A., 2013. Capillaroscopy in psoriatic and rheumatoid arthritis: a useful tool for differential diagnosis. Arthritis 2013 (1), 957480. https://doi.org/10.1155/2013/957480.
[40] Hofstee, H., De Waal, T., Zweegman, S., Voskuyl, A., Smulders, Y., Schoordijk, M., Janssen, J., Serné, E., 2013. Nailfold capillary abnormalities in sclerodermatous chronic GVHD. Bone Marrow Transpl 48 (12), 1574–1577. https://doi.org/10.1038/bmt.2013.106.
[41] Deng, Y., Zhang, Y., Lemos, B., Ren, H., 2017. Tissue accumulation of microplastics in mice and biomarker responses suggest widespread health risks of exposure. Sci Rep 7, 46687. https://doi.org/10.1038/srep46687.
[42] Lin, S., Zhang, H., Wang, C., Su, X.-L., Song, Y., Wu, P., Yang, Z., Wong, M.-H., Cai, Z., Zheng, C., 2022. Metabolomics reveal nanoplastic-induced mitochondrial damage in human liver and lung cells. Environ Sci Technol 56 (17), 12483–12493. https://doi.org/10.1021/acs.est.2c03980.
[43] Poon, W., Zhang, Y.-N., Ouyang, B., Kingston, B.R., Wu, J.L., Wilhelm, S., Chan, W. C., 2019. Elimination pathways of nanoparticles. ACS Nano 13 (5), 5785–5798. https://doi.org/10.1021/acsnano.9b01383.
[44] Stater, E.P., Sonay, A.Y., Hart, C., Grimm, J., 2021. The ancillary effects of nanoparticles and their implications for nanomedicine. Nat Nanotechnol 16 (11), 1180–1194. https://doi.org/10.1038/s41565-021-01017-9.
[45] Hu, Y., Shen, M., Wang, C., Huang, Q., Li, R., Dorj, G., Gombojav, E., Du, J., Ren, L., 2024. A meta-analysis-based adverse outcome pathway for the Male reproductive toxicity induced by microplastics and nanoplastics in mammals. J Hazard Mater 465, 133375. https://doi.org/10.1016/j.jhazmat.2023.133375.
[46] Monikh, F.A., Lehtonen, Š., Kekäläinen, J., Karkossa, I., Auriola, S., Schubert, K., Zanut, A., Peltonen, S., Niskanen, J., Bandekar, M., 2024. Biotransformation of nanoplastics in human plasma and their permeation through a model in vitro blood-brain barrier: an in-depth quantitative analysis. Nano Today 59, 102466. https://doi.org/10.1016/j.nantod.2024.102466.
[47] Saab, Y., Oueis, E., Mehanna, S., Nakad, Z., Stephan, R., Khnayzer, R.S., 2022. Risk assessment of phthalates and their metabolites in hospitalized patients: a focus on di-and mono-(2-ethylhexyl) phthalates exposure from intravenous plastic bags. Toxics 10 (7), 357. https://doi.org/10.3390/toxics10070357.
[48] Štrac, I.V., Pušić, M., Gajski, G., Garaj-Vrhovac, V., 2013. Presence of phthalate esters in intravenous solution evaluated using gas chromatography–mass spectrometry method. J Appl Toxicol 33 (3), 214–219. https://doi.org/10.1002/jat.1741.
[49] Ong, H., Samsudin, H., SotoValdez, H., 2022. Migration of endocrine-disrupting chemicals into food from plastic packaging materials: an overview of chemical risk assessment, techniques to monitor migration, and international regulations. Crit Rev Food Sci 62 (4), 957–979. https://doi.org/10.1080/10408398.2020.1830747.
[50] Gahleitner, M., Paulik, C., 2017. Brydson's plastics materials. Elsevier, pp. 279–309. https://doi.org/10.1016/B978-0-323-35824-8.00011-6.
[51] Gosetti, F., Bolfi, B., Robotti, E., Manfredi, M., Binotti, M., Ferrero, F., Bona, G., Marengo, E., 2018. Study of endocrine disrupting compound release from different medical devices through an on-line SPE UHPLC-MS/MS method. Anal Chim Acta 1042, 141–154. https://doi.org/10.1016/j.aca.2018.07.028.
[52] Prasad, B., Prasad, K.S., Dave, H., Das, A., Asodariya, G., Talati, N., Swain, S., Kapse, S., 2022. Cumulative human exposure and environmental occurrence of phthalate esters: a global perspective. Environ Res 210, 112987. https://doi.org/10.1016/j.envres.2022.112987.
[53] Kay, V.R., Bloom, M.S., Foster, W.G., 2014. Reproductive and developmental effects of phthalate diesters in males. Crit Rev Toxicol 44 (6), 467–498. https://doi.org/10.3109/10408444.2013.875983.
[54] Liu, L., Li, X., Luo, X., Wang, X., Liu, L., Yuan, Z., Sun, C., Zheng, H., Xu, E.G., Li, F., 2025. Phthalates esters disrupt demersal fish behavior: unveiling the brain-gut axis impact. Ecotox Environ Safe 289, 117470. https://doi.org/10.1016/j.ecoenv.2024.117470.
[55] Meng, M., Yang, Y., Song, L., Peng, J., Li, S., Gao, Z., Bu, Y., Gao, J., 2024. Association between urinary phthalates and phthalate metabolites and cancer risk: a systematic review and meta-analysis. Heliyon. https://doi.org/10.1016/j.heliyon.2024.e29684.
[56] EFSA Panel on Food Contact Materials, E., Aids, P., Silano, V., Barat Baviera, J.M., Bolognesi, C., Chesson, A., Cocconcelli, P.S., Crebelli, R., Gott, D.M., Grob, K., Lampi, E., 2019. Update of the risk assessment of di-butylphthalate (DBP), butyl-benzyl-phthalate (BBP), bis (2-ethylhexyl) phthalate (DEHP), di-isononylphthalate (DINP) and di-isodecylphthalate (DIDP) for use in food contact materials. EFSA J 17 (12), e05838. https://doi.org/10.2903/j.efsa.2019.5838.
[57] Liu, H., Zheng, D., Liu, X., Hou, J., Wu, Q., Li, Y., 2024. Environmental microplastic and phthalate esters co-contamination, interrelationships, co-toxicity and mechanisms. A review. Environ Geochem Hlth 46 (12), 525. https://doi.org/10.1007/s10653-024-02309-4.
[58] Gao, M., Bai, L., Xiao, L., Peng, H., Chen, Q., Qiu, W., Song, Z., 2024. Micro (nano) plastics and phthalate esters drive endophytic bacteria alteration and inhibit wheat root growth. Sci Total Environ 906, 167734. https://doi.org/10.1016/j.scitotenv.2023.167734.
[59] Zhang, J., Li, D., Lu, C., Wang, X., Wang, J., Wang, J., Li, B., Du, Z., Yang, Y., Zhu, L., 2024. Negative effects of polyvinyl chloride microplastics and the plasticizer DnOP on earthworms: Co-exposure enhances oxidative stress and immune system damage in earthworms. J Hazard Mater 480, 136338. https://doi.org/10.1016/j.jhazmat.2024.136338.
[60] Kik, K., Bukowska, B., Sicińska, P., 2020. Polystyrene nanoparticles: sources, occurrence in the environment, distribution in tissues, accumulation and toxicity to various organisms. Environ Pollut 262, 114297. https://doi.org/10.1016/j.envpol.2020.114297.
[61] Li, B., Li, M., Du, D., Tang, B., Yi, W., He, M., Liu, R., Yu, H., Yu, Y., Zheng, J., 2025. Characteristics and influencing factors of microplastics entering human blood through intravenous injection. Environ Int 198, 109377. https://doi.org/10.1016/j.envint.2025.109377.
[62] Zhang, X., Li, N., Li, X., Liu, C., Wang, M., Zhang, S., Dong, Z., Ma, J., Liu, S., 2025. Reactive oxygen species drive aging-associated microplastic release in diverse infusion ingredients. J Hazard Mater 490, 137728. https://doi.org/10.1016/j.jhazmat.2025.137728.